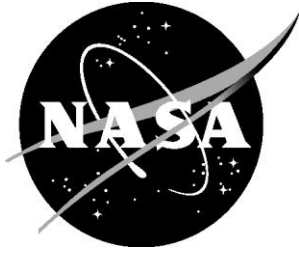


NASA/TM-2020-5002898



A Method for Correlating Forward-Looking Remote Sensor Measurements with In-Situ Measurements on Flying Platforms

Justin K. Strickland
Analytical Mechanics Associates, Inc., Hampton, Virginia

Patricia J. Hunt
Analytical Mechanics Associates, Inc., Hampton, Virginia

Steven D. Harrah
Langley Research Center, Hampton, Virginia

George F. Switzer
Analytical Mechanics Associates, Inc., Hampton, Virginia

NASA STI Program . . . in Profile

Since its founding, NASA has been dedicated to the advancement of aeronautics and space science. The NASA scientific and technical information (STI) program plays a key part in helping NASA maintain this important role.

The NASA STI program operates under the auspices of the Agency Chief Information Officer. It collects, organizes, provides for archiving, and disseminates NASA's STI. The NASA STI program provides access to the NTRS Registered and its public interface, the NASA Technical Reports Server, thus providing one of the largest collections of aeronautical and space science STI in the world. Results are published in both non-NASA channels and by NASA in the NASA STI Report Series, which includes the following report types:

- **TECHNICAL PUBLICATION.** Reports of completed research or a major significant phase of research that present the results of NASA Programs and include extensive data or theoretical analysis. Includes compilations of significant scientific and technical data and information deemed to be of continuing reference value. NASA counter-part of peer-reviewed formal professional papers but has less stringent limitations on manuscript length and extent of graphic presentations.
- **TECHNICAL MEMORANDUM.** Scientific and technical findings that are preliminary or of specialized interest, e.g., quick release reports, working papers, and bibliographies that contain minimal annotation. Does not contain extensive analysis.
- **CONTRACTOR REPORT.** Scientific and technical findings by NASA-sponsored contractors and grantees.

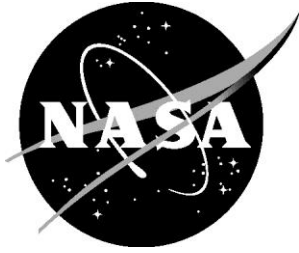
- **CONFERENCE PUBLICATION.** Collected papers from scientific and technical conferences, symposia, seminars, or other meetings sponsored or co-sponsored by NASA.
- **SPECIAL PUBLICATION.** Scientific, technical, or historical information from NASA programs, projects, and missions, often concerned with subjects having substantial public interest.
- **TECHNICAL TRANSLATION.** English-language translations of foreign scientific and technical material pertinent to NASA's mission.

Specialized services also include organizing and publishing research results, distributing specialized research announcements and feeds, providing information desk and personal search support, and enabling data exchange services.

For more information about the NASA STI program, see the following:

- Access the NASA STI program home page at <http://www.sti.nasa.gov>
- E-mail your question to help@sti.nasa.gov
- Phone the NASA STI Information Desk at 757-864-9658
- Write to:
NASA STI Information Desk
Mail Stop 148
NASA Langley Research Center
Hampton, VA 23681-2199

NASA/TM-2020-5002898



A Method for Correlating Forward-Looking Remote Sensor Measurements with In-Situ Measurements on Flying Platforms

Justin K. Strickland
Analytical Mechanics Associates, Inc., Hampton, Virginia

Patricia J. Hunt
Analytical Mechanics Associates, Inc., Hampton, Virginia

Steven D. Harrah
Langley Research Center, Hampton, Virginia

George F. Switzer
Analytical Mechanics Associates, Inc., Hampton, Virginia

National Aeronautics and
Space Administration

Langley Research Center
Hampton, Virginia 23681-2199

June 2020

The use of trademarks or names of manufacturers in this report is for accurate reporting and does not constitute an official endorsement, either expressed or implied, of such products or manufacturers by the National Aeronautics and Space Administration.

Available from:

NASA STI Program / Mail Stop 148
NASA Langley Research Center
Hampton, VA 23681-2199
Fax: 757-864-6500

Abstract

A method is described for correlating measurements from a forward looking remote sensor with measurements made by in-situ instruments installed on the same flying platform. This method assumes that remote measurements are made within a volume of space in advance of the aircraft and that in-situ measurements provide representative values for discrete segments along the flight path. This correlation method can be applied to multiple sensors and makes no assumptions about the type of remote sensor or in-situ instrument, nor what either measures. It may be applied to recorded data during post-flight analysis based on known 4-D location (geospacial position and time) measurements.

Introduction

Flight test campaigns often outfit an aircraft with a variety of instruments to collect scientific measurements in addition to recording measurements available from standard avionics equipment via an avionics data bus. Some of these instruments might be remote sensors such as radar or lidar which measure conditions at a distance from the aircraft, while others such as pitot probes or temperature sensors measure conditions at the aircraft position (i.e. in-situ). A remote forward looking sensor measures in advance of the aircraft; if any of these remote measurements are along the subsequent flight path, they will be associated with in-situ measurements. The in-situ measurements then can serve as a validation and/or correlation of the remote measurements. The two NASA/FAA High Ice Water Content (HIWC) Radar flight campaigns [1, 2] utilized this scenario, during which an airborne weather radar operated in normal weather mode scanning a volume of space ahead of the aircraft while fuselage- and wing-mounted probe instruments collected in-situ measurements as the aircraft subsequently flew through specific regions of the scanned volume. A primary goal of the flight campaigns was to correlate the remote radar measurements with in-situ measurements to assess estimates of weather conditions at remote ranges with the actual sampled conditions [3, 4].

The purpose of the in-situ measurements is to validate the accuracy of the remote measurements by sampling the same airspace at a time after the remote measurement has occurred. In operations, the benefit of remote measurements is to inform the flight crew about conditions far enough in front of the aircraft to provide adequate warning to be able to maneuver around or to secure the cabin for adverse environmental conditions. Therefore, remote sensor performance is assessed at some distance ahead of the aircraft.

The correlation process is agnostic regarding the type and output of remote and in-situ instruments. It merely relates specific measurements from a remote sensor (scanning or fixed) with the in-situ measurements taken along a non-linear flight path. The nature of the correlation involves identifying where remote and in-situ measurements occur at the same spatial location (albeit at different times). It also accounts for earth curvature, which becomes significant at long ranges. The correlation process presented here demonstrates a method to match the disparate distance and size scales of the remote and in-situ instruments.

A description of the correlation process follows. Because this is largely a geometry problem, the process makes use of several coordinate systems and their related transformations. These are defined first, followed by a description of the algorithm that identifies candidate remote measurements. Finally, the correlation description concludes with the filtering process of all candidate remote measurements to compute one representative remote measurement with similar distance scale for each in-situ measurement.

Reference Frames

There are two types of reference frames used to perform the correlation: Earth-centered coordinate systems rotating with the Earth, and observer-centered coordinate systems that translate and rotate with the rotation of the Earth and the motion of an observer relative to the surface of the Earth. The reference frames apply to both Cartesian and spherical coordinate systems. The source code used to compute the reference frame transformations is publicly available [5, 6] and is described in the Appendix.

Earth-Centered Reference Frames

The correlation process uses two Earth-centered reference frames defined in the World Geodetic System 1984 (WGS84) standard [7]. The first is the Earth-Centered-Fixed (ECF) – also known as Earth-Centered-Earth-Fixed (ECEF) – reference frame which is a geocentric right-handed Cartesian coordinate system with the X-Y plane coplanar with the Earth's equatorial plane, the Z-axis passing through the North Pole, and the X-axis passing through the intersection of the equator and prime meridian (0° latitude, 0° longitude). The second is the Latitude-Longitude-Altitude (LLA) reference frame which is a geodetic spherical coordinate system where the altitude (h) is relative to a reference ellipsoid (Figure 1).

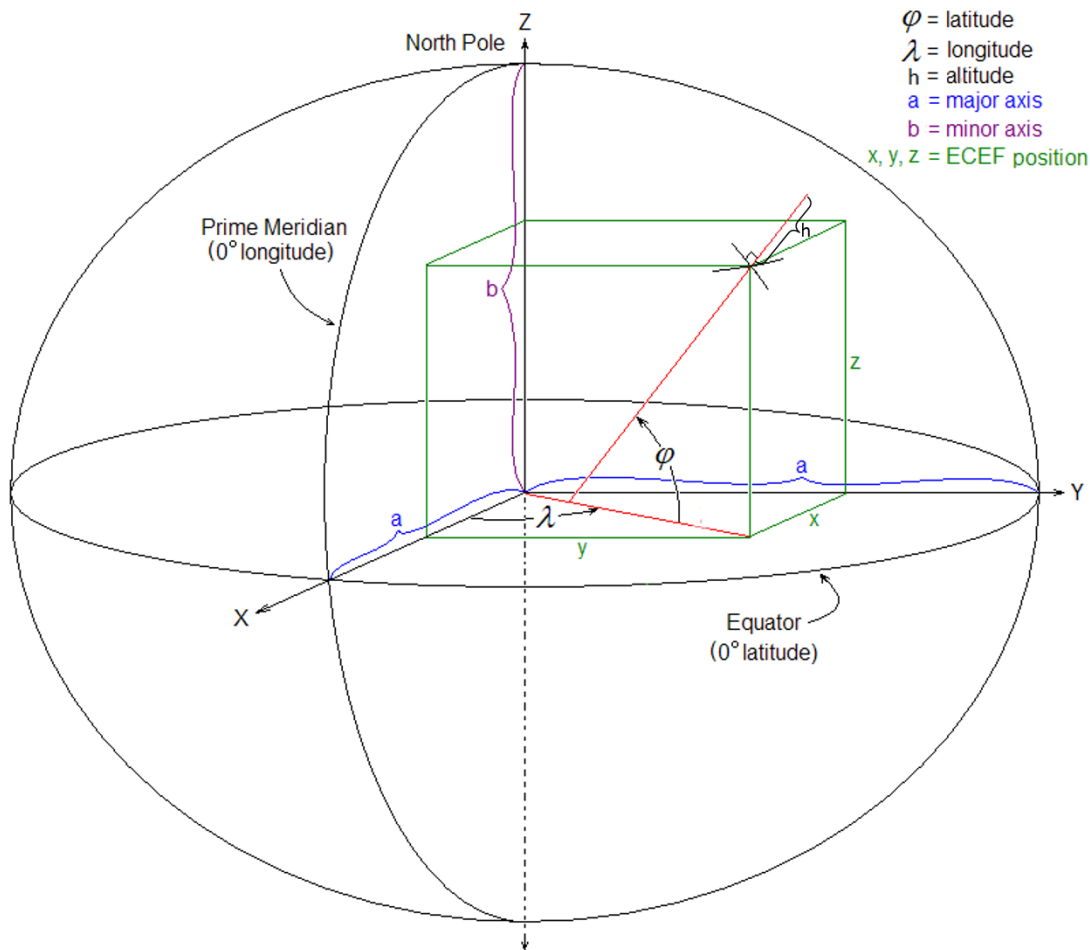


Figure 1: Earth-Centered Coordinate Systems. [Public Domain¹]

¹ Based on en:File:ECEF.png by Wikimedia user Kr7cmw01 <https://commons.wikimedia.org/wiki/File:ECEF.png>

The global positioning system (GPS) uses the WGS84 standard and navigation systems commonly report geodetic LLA positions from GPS receivers, therefore, converting positions into geocentric ECF coordinates provides a means of computing position differences. The conversion from LLA (coordinates: φ , λ and h) to ECF (coordinates: x , y , and z) is given by [7]:

$$x = (N + h) \cos \varphi \cos \lambda \quad (1.1)$$

$$y = (N + h) \cos \varphi \sin \lambda \quad (1.2)$$

$$z = \left[\left(\frac{b^2}{a^2} \right) N + h \right] \sin \varphi \quad (1.3)$$

where:

$$N = \frac{a}{\sqrt{1 - e^2 \sin^2 \varphi}} \quad (1.4)$$

$$e^2 = 1 - \frac{b^2}{a^2} \quad (1.5)$$

$$a = 6378137.0 \text{ meters}$$

$$b = 6356752.3142 \text{ meters}$$

$$e = 8.1819190842622 \times 10^{-2}$$

No closed form solution exists for the inverse conversion from geocentric ECF to geodetic LLA, however there are iterative solutions for the inverse conversion that account for the singularities at the poles. The correlation process does not require the inverse conversion to be made. However, for completeness a solution is implemented in the source code described in the Appendix.

Observer-Centered Reference Frames

There are three observer-centered reference frames used to determine the location of remote measurements relative to an observer (i.e. remote sensor): East-North-Up (ENU), Downrange-Crossrange-Above (DCA), and Azimuth-Elevation-Range (AER).

The first, East-North-Up (ENU), is a right-handed Cartesian coordinate system with the origin at the observer position where the E-N plane represents the local horizon (i.e. tangent to the reference ellipsoid), the U-axis aligns with the local vertical direction, and the N-axis aligns with true north (Figure 2).

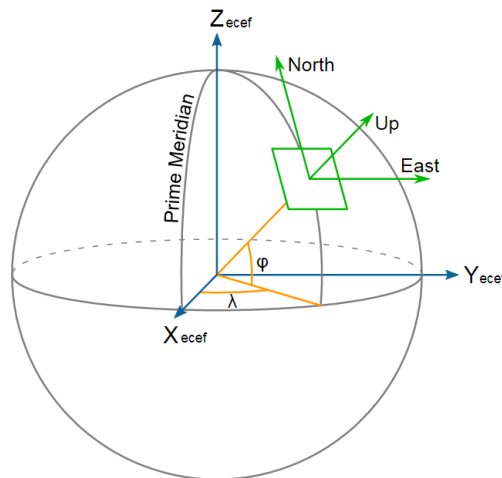


Figure 2: East-North-Up Observer-Centered Coordinate System. [Public Domain²]

² Created by Wikimedia user Mike1024 - Based on en:File:EarthTangentialPlane.png by en:User:Raffy199 https://commons.wikimedia.org/wiki/File:ECEF_ENU_Longitude_Latitude_relationships.svg

The second reference frame accounts for the forward-facing direction of the observer, which is specified by the true heading of a flying platform. The Downrange-Crossrange-Above (DCA) reference frame is a right-handed Cartesian coordinate system where the D-C plane is coplanar with the E-N plane (local horizontal), the A-axis is congruent with the U-axis (local vertical), and the D-axis aligns with the aircraft true heading (Ψ) (Figure 3). Compass heading must be corrected for magnetic declination and compass deviation to true heading to properly define the DCA reference frame. Furthermore, the orientation of the flight vehicle does not necessarily align with the DCA coordinates.

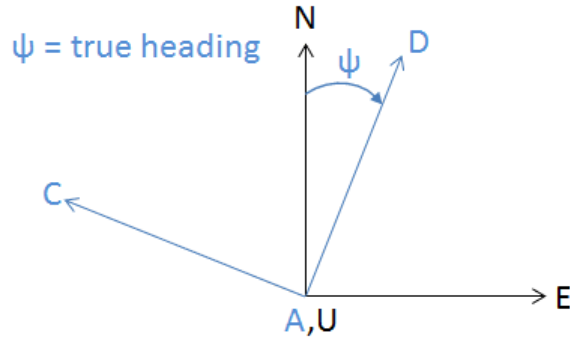


Figure 3: Downrange-Crossrange-Above Observer-Centered Coordinate System (Overhead View).

The conversions between the ENU and DCA coordinate systems is given by:

$$\begin{bmatrix} D \\ C \\ A \end{bmatrix} = \begin{bmatrix} \sin \psi & \cos \psi & 0 \\ -\cos \psi & \sin \psi & 0 \\ 0 & 0 & 1 \end{bmatrix} \begin{bmatrix} E \\ N \\ U \end{bmatrix} \quad (2)$$

The conversions between the DCA and ENU coordinate systems is given by³:

$$\begin{bmatrix} E \\ N \\ U \end{bmatrix} = \begin{bmatrix} \sin \psi & -\cos \psi & 0 \\ \cos \psi & \sin \psi & 0 \\ 0 & 0 & 1 \end{bmatrix} \begin{bmatrix} D \\ C \\ A \end{bmatrix} \quad (3)$$

The third reference frame allows for specifying positions that are not directly in front of the observer by angles relative to the forward-facing direction (i.e. measured from the true heading direction of the platform). The Azimuth-Elevation-Range (AER) reference frame is a spherical coordinate system where the azimuth angle (ϕ) specifies the horizontal rotation measured from the D-axis of the DCA coordinate system (positive toward starboard or clockwise when viewed from above), the elevation angle (θ) specifies the vertical rotation measured from the horizontal plane (positive upward), and the range (R) is the slant range to a specified position (Figure 4). By these definitions, the azimuth and elevation angles represent extrinsic Euler angle rotations.

³ Note that direction cosine matrices (DCM) are orthogonal matrices, meaning the matrix's inverse is equal to its transpose.

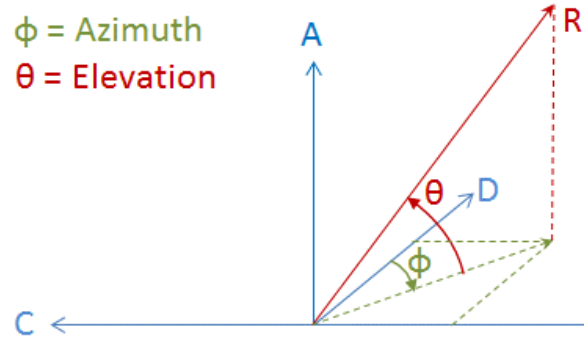


Figure 4: Azimuth-Elevation-Range Observer-Centered Coordinate System.

The conversion from the AER (coordinates: ϕ , θ , and R) coordinate system to the DCA coordinate system is given by:

$$D = R \cos \phi \cos \theta \quad (4.1)$$

$$C = -R \sin \phi \cos \theta \quad (4.2)$$

$$A = R \sin \theta \quad (4.3)$$

The conversion from the DCA coordinate system to the AER coordinate system is given by:

$$\phi = \tan^{-1} \left(\frac{-C}{D} \right) \quad (5.1)$$

$$\theta = \tan^{-1} \left(\frac{A}{\sqrt{D^2 + C^2}} \right) \quad (5.2)$$

$$R = \sqrt{D^2 + C^2 + A^2} \quad (5.3)$$

Singularities exist when the elevation angle (θ) is $\pm 90^\circ$ causing the azimuth angle (ϕ) to be undefined, and the singularities should be accounted for using conditional logic in a software implementation.

For an aircraft with a remote sensor installed looking forward, the sensor boresight aligns with the downrange axis. For a scanning remote sensor the azimuth and elevation angles account for the boresight offset from the downrange axis in the DCA coordinate system. Sensor systems employing elevation-over-azimuth 2-axis gimbal positioners conform to these definitions whereas azimuth-over-elevation positioners do not. Azimuth and elevation are not necessarily equivalent to the positioner gimbal angles due to platform orientation relative to the DCA and AER coordinate systems. Remote sensor systems may compensate for aircraft pitch and roll and report the corresponding azimuth and elevation angles, otherwise the azimuth and elevation angles must be computed from the positioner gimbal, aircraft pitch, and aircraft roll angles. Likewise, the AER coordinate system may be used to compensate for aircraft pitch via elevation angle for remote sensor systems with boresight directions fixed (e.g. non-scanning) straight ahead of the platform.

Conversion Between Earth-Centered and Observer-Centered Reference Frames

The bridge between the Earth-centered and observer-centered reference frames is via the conversions between the ECF and ENU coordinate systems. The conversion requires knowing the origin of the ENU reference frame relative to an Earth-centered reference frame. The conversion from the ECF coordinate system to the ENU coordinate system is given by:

$$\begin{bmatrix} E \\ N \\ U \end{bmatrix} = \begin{bmatrix} -\sin \lambda_o & \cos \lambda_o & 0 \\ -\sin \varphi_o \cos \lambda_o & -\sin \varphi_o \sin \lambda_o & \cos \varphi_o \\ \cos \varphi_o \cos \lambda_o & \cos \varphi_o \sin \lambda_o & \sin \varphi_o \end{bmatrix} \begin{bmatrix} x - x_o \\ y - y_o \\ z - z_o \end{bmatrix} \quad (6)$$

where φ_o and λ_o are the geodetic latitude and longitude of the origin of the ENU reference frame in the LLA reference frame, $\{x, y, z\}$ is the position in the ECF reference frame, and $\{x_o, y_o, z_o\}$ is the position of the origin of the ENU reference frame in the ECF reference frame.

Using the same variable definitions as above, the reverse conversion from the ENU coordinate system to the ECF coordinate system is given by³:

$$\begin{bmatrix} x \\ y \\ z \end{bmatrix} = \begin{bmatrix} -\sin \lambda_o & -\sin \varphi_o \cos \lambda_o & \cos \varphi_o \cos \lambda_o \\ \cos \lambda_o & -\sin \varphi_o \sin \lambda_o & \cos \varphi_o \sin \lambda_o \\ 0 & \cos \varphi_o & \sin \varphi_o \end{bmatrix} \begin{bmatrix} E \\ N \\ U \end{bmatrix} + \begin{bmatrix} x_o \\ y_o \\ z_o \end{bmatrix} \quad (7)$$

where $\{E, N, U\}$ is the position in the ENU reference frame.

Measurement Correlation

The goal of the measurement correlation between a remote sensor and an in-situ instrument is to produce comparable measurements of the same location. This correlation is complicated by differences in both time and volume measured by each system. Platform based forward-looking remote sensors measure conditions that in-situ instruments measure at some subsequent time. This time delay complicates the comparative process. A scanning remote sensor – especially one with a widening beam such as radar – produces measurements of a large volume compared to the point measurements from in-situ instruments flying through that same airspace. Therefore, the correlation process must properly filter remote measurements to arrive at the subset of those representative of known aircraft positions. These filtered remote measurements will be referred to as candidate measurements to distinguish them for further processing.

Another complicating factor is the likely disparity in remote sensor and in-situ instrument sample volumes. Remote sensor measurement volumes may exceed a cubic kilometer of sky only a short distance ahead of the aircraft. Whereas in-situ instrument measurements are produced by sampling a small cross-sectional area – often on the order of square centimeters – but can result in integrated/averaged values for sample paths up to kilometers in length/duration. These sample volume disparities increase the spatial complication of the comparisons. However, in spite of this complexity this analysis process assumes in-situ measurements represent point measurements made at specific intervals along the flight path.

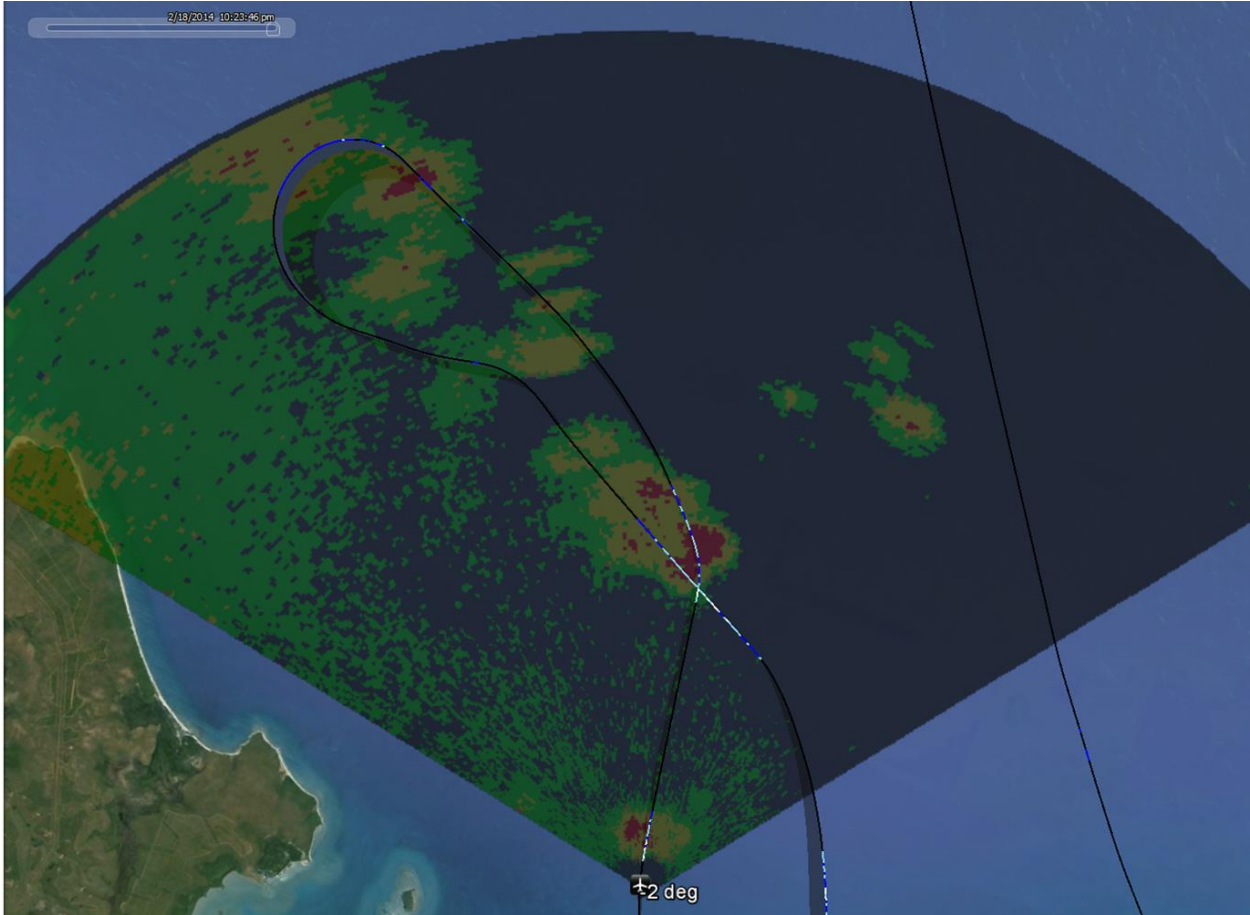


Figure 5: Example Showing Remote Measurements Represented by a Radar PPI Image and In-situ Measurements Represented by the Color-Coded Flight Path

For example, Figure 5 illustrates a remote measurement volume represented by a radar plan-position indicator (PPI) image of a scan color-coded by radar reflectivity factor (RRF). Likewise, the ensuing flight path is color-coded according to measurements made by an in-situ instrument (value and duration). Also shown (the black line to the right) is a segment of flight path from a much later time.

Compute Line-of-Sight Vectors

The measurement correlation process needs to develop associations for remote sensor measurements corresponding to aircraft positions along the flight path measured by the in-situ instrument(s). This association process determines when an in-situ measurement falls within a remote measurement resolution volume by first computing line-of-sight (LOS) vectors originating from the aircraft position at the time of the remote measurement to all subsequent in-situ measurement positions (Figure 6). This is done by defining the origin of an ENU reference frame at the starting aircraft position (given by LLA coordinates) and converting each in-situ measurement position from LLA coordinates, to ECF coordinates, to ENU coordinates. This specific order ensures the correct representation of a position and makes use of the ECF to ENU bridge between earth-centered and observer-centered reference frames. The resulting LOS vector in the ENU reference frame is given by combining equation 1 with equation 6:

$$\overline{LOS} = \begin{bmatrix} -\sin \lambda_o & \cos \lambda_o & 0 \\ -\sin \varphi_o \cos \lambda_o & -\sin \varphi_o \sin \lambda_o & \cos \varphi_o \\ \cos \varphi_o \cos \lambda_o & \cos \varphi_o \sin \lambda_o & \sin \varphi_o \end{bmatrix} \begin{bmatrix} (N_m + h_m) \cos \varphi_m \cos \lambda_m - (N_o + h_o) \cos \varphi_o \cos \lambda_o \\ (N_m + h_m) \cos \varphi_m \sin \lambda_m - (N_o + h_o) \cos \varphi_o \sin \lambda_o \\ \left[\left(\frac{b^2}{a^2} \right) N_m + h_m \right] \sin \varphi_m - \left[\left(\frac{b^2}{a^2} \right) N_o + h_o \right] \sin \varphi_o \end{bmatrix} \quad (8.1)$$

where:

$$N_m = \frac{a}{\sqrt{1 - e^2 \sin^2 \varphi_m}} \quad (8.2)$$

$$N_o = \frac{a}{\sqrt{1 - e^2 \sin^2 \varphi_o}} \quad (8.3)$$

$\{\varphi_o, \lambda_o, h_o\}$ is the geodetic latitude, longitude, and altitude of the position from which the remote measurement is made and $\{\varphi_m, \lambda_m, h_m\}$ is the geodetic latitude, longitude, and altitude of an in-situ measurement position.

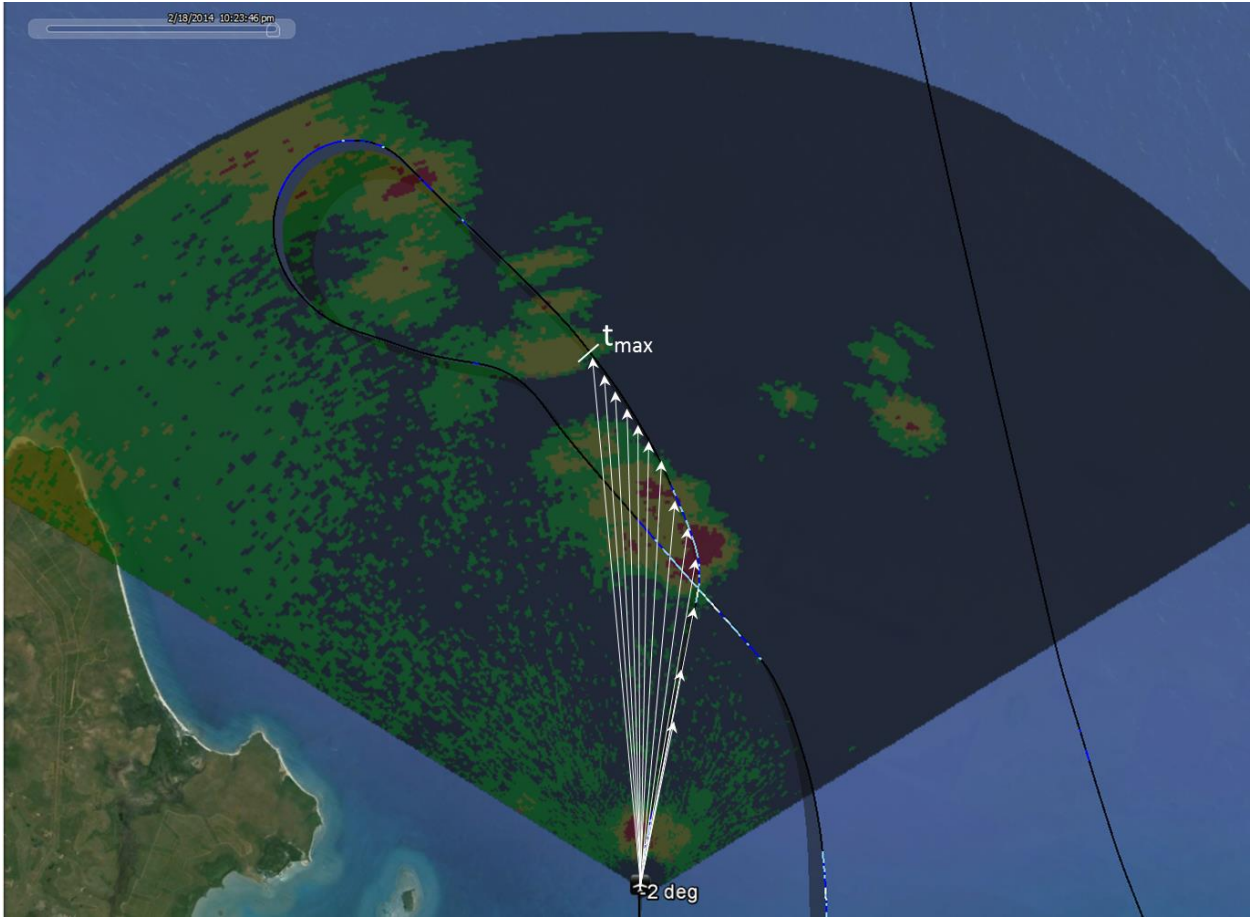


Figure 6: Example Line-of-Sight Vectors Starting at a Position From Which Remote Measurements Were Made to All Subsequent In-situ Measurement Positions (within time limit).

Because the platform flight paths are not necessarily straight lines but may loop around, the aircraft may pass through or near the same location multiple times, sometimes separated by hours. Therefore, to associate valid remote and in-situ measurements, the association process imposes a maximum time limit between in-situ and remote measurement positions. This insures that later transits of the same space are not associated with an earlier and unrelated remote measurement. The ratio of the maximum desirable remote measurement range and the aircraft true airspeed (i.e., $t_{max} \approx R_{max}/TAS$) determines the time limit.

Determine Remote and In-situ Measurement Associations

The correlation process to determine candidate measurement associations accounts for angle (boresight direction and beamwidth) and range resolution of the remote sensor. For a given remote sensor measurement, each LOS vector is compared with the remote sensor's boresight pointing direction to determine those falling within the remote sensor's beamwidth (Figure 7). Their magnitudes determine which range resolution volume of the remote measurements to associate with their corresponding in-situ measurement.

If the resolution volume of the remote sensor is greater than the distance separating several in-situ measurements, then a single remote measurement value may be associated with multiple in-situ measurements. Conversely, for a scanning remote sensor with azimuth steps less than the beamwidth, the overlapping beams result in multiple remote measurement associations with a single in-situ measurement. The resulting candidate measurement associations capture every remote measurement made at each in-situ measurement position up to the specified time limit (t_{max}). The process discards all other remote measurements and is repeated for every remote sensor measurement.

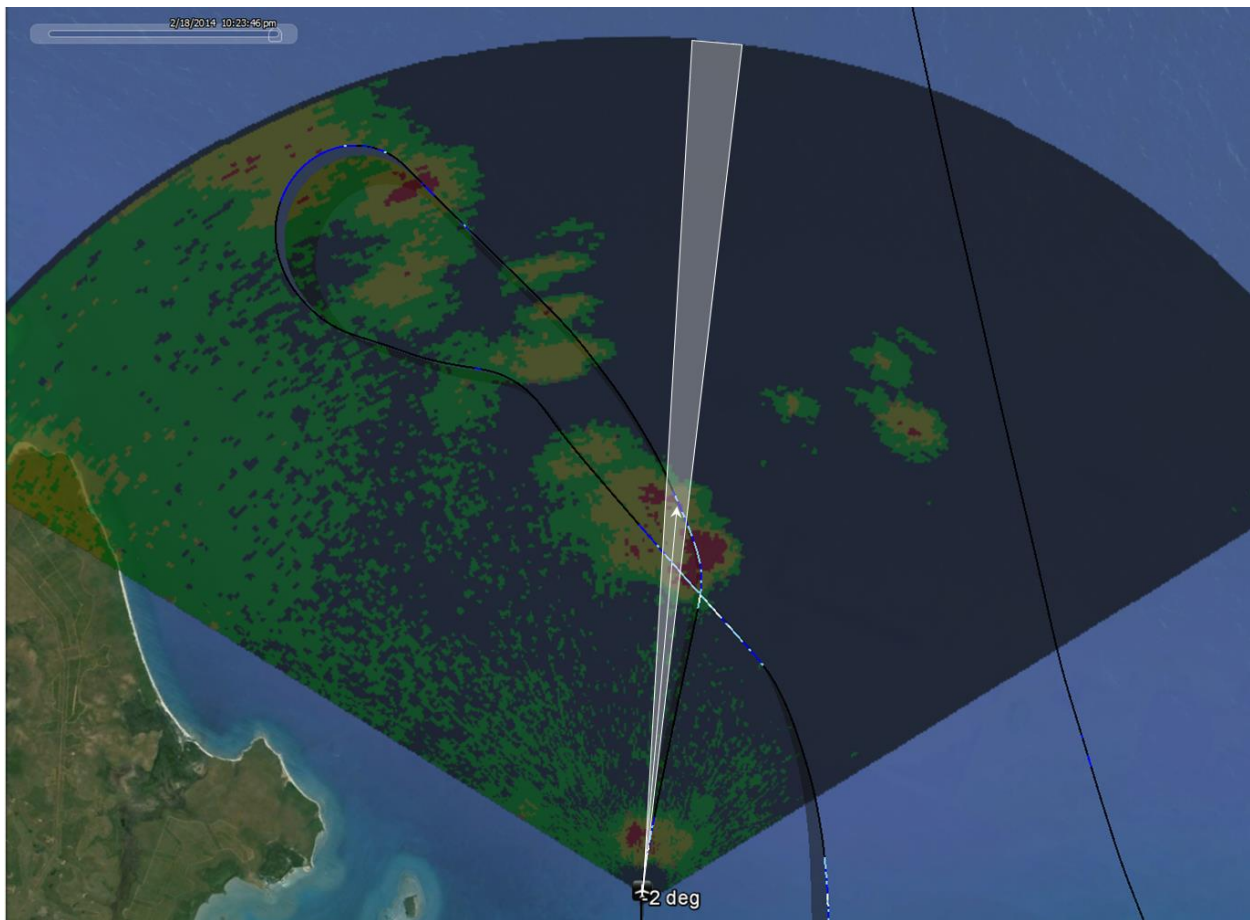


Figure 7: Example of Line-of-Sight Vector Within Remote Sensor Beamwidth

The remote sensor can have any beam shape. Assuming a symmetrical/conical beam shape, the beamwidth is specified by a single angle. If the compound angle between the LOS vector and the sensor boresight is less than half the beamwidth, then the in-situ measurement is within the remote measurement volume.

The compound angle may be determined by computing the dot product of the LOS vector with the sensor boresight vector (\vec{R}) in a common Cartesian reference frame. It is convenient to convert both into the DCA reference frame (LOS from ENU to DCA using equation 2 and boresight from AER to DCA using equation 4) such that the compound angle is given by:

$$\Theta = \cos^{-1} \left(\frac{\overline{LOS} \cdot \vec{R}}{|\overline{LOS}| |\vec{R}|} \right) \quad (9)$$

where \overline{LOS} and \vec{R} are represented by DCA coordinates.

Alternatively, if the LOS vector is converted into the AER spherical reference frame using equations 2 and 5, the compound angle is given by:

$$\Theta = \cos^{-1} [\cos \theta_m \cos \theta_b \cos(\phi_m - \phi_b) + \sin \theta_m \sin \theta_b] \quad (10)$$

where ϕ_m and θ_m are the azimuth and elevation angles respectively to the subsequent in-situ measurement position and ϕ_b and θ_b are the azimuth and elevation angles respectively of the remote sensor boresight direction.

Non-symmetrical beam shapes require a different relationship. The singularities that exist at elevation angles (θ) of $\pm 90^\circ$ are unlikely to be encountered in this process because in-situ measurements are not collected directly above or below the platform unless the aircraft flies vertically, nor are forward looking remote sensors expected to tilt vertically.

Filter by Range

A remote scanning sensor can employ a scan pattern that covers a large volume, so only those boresight angles that encompass in-situ measurement(s) within a resolution volume will be acceptable to derive candidate associations. The remote sensor's scan pattern may result in associations for a given in-situ measurement with remote measurements from any range between the minimum range of the remote sensor to the farthest LOS vector position near the time limit, which may be separated by several kilometers. The candidate remote measurements are filtered by range to facilitate evaluating remote sensor performance as a function of range. Each in-situ measurement position may be sampled during multiple remote sensor scans separated significantly in time. Due to aircraft motion, each scan of the remote sensor represents a different range to a given in-situ measurement. Therefore, a range window is used to increase the number of acceptable associations that relate to a specific in-situ measurement. Consequently, the candidate remote measurements are filtered by range to discard any that do not meet a pre-defined range window specified by R_{\min} and R_{\max} (Figure 8).

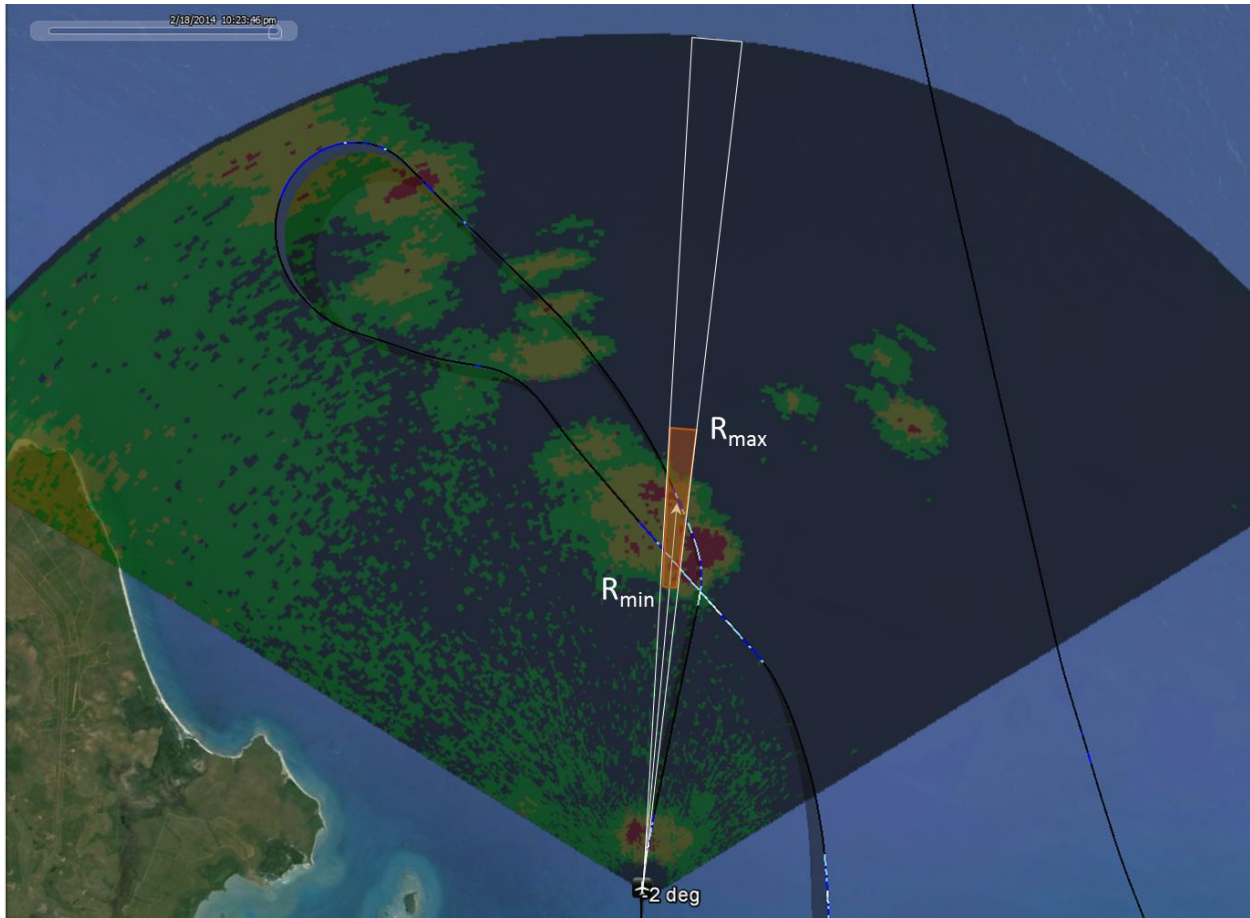


Figure 8: Example of Filtering Candidate Remote Measurement by Pre-defined Range Window

Depending on the volumetric scan pattern performed by the remote sensor, the remote sensor beam may not revisit a given location every sweep, and maybe only once per volume scan. The range window must be chosen to maximize the number of possible remote measurement samples while concentrating samples near the desired range. For example, assuming a 10 km wide range window, the correlation process may include only candidate remote measurements from 0 to 10 km in range to evaluate remote sensor measurements made near the aircraft. Similarly, specifying a range window from 40 to 50 km in range results in correlations representative of remote sensor measurements at a nominal 45 km distance.

A Unified Modeling Language (UML) [8] activity diagram (Figure 9) provides an overview of the described association process by outlining an algorithm. Depending on the structure of the (remote and in-situ) measurement data, additional logic might be added to an implementation of this algorithm for efficiency gains. For example, if the measurement data is ordered chronologically, the inner loop is easily truncated by the time limits. Likewise, the outer loop might be similarly truncated by the range window.

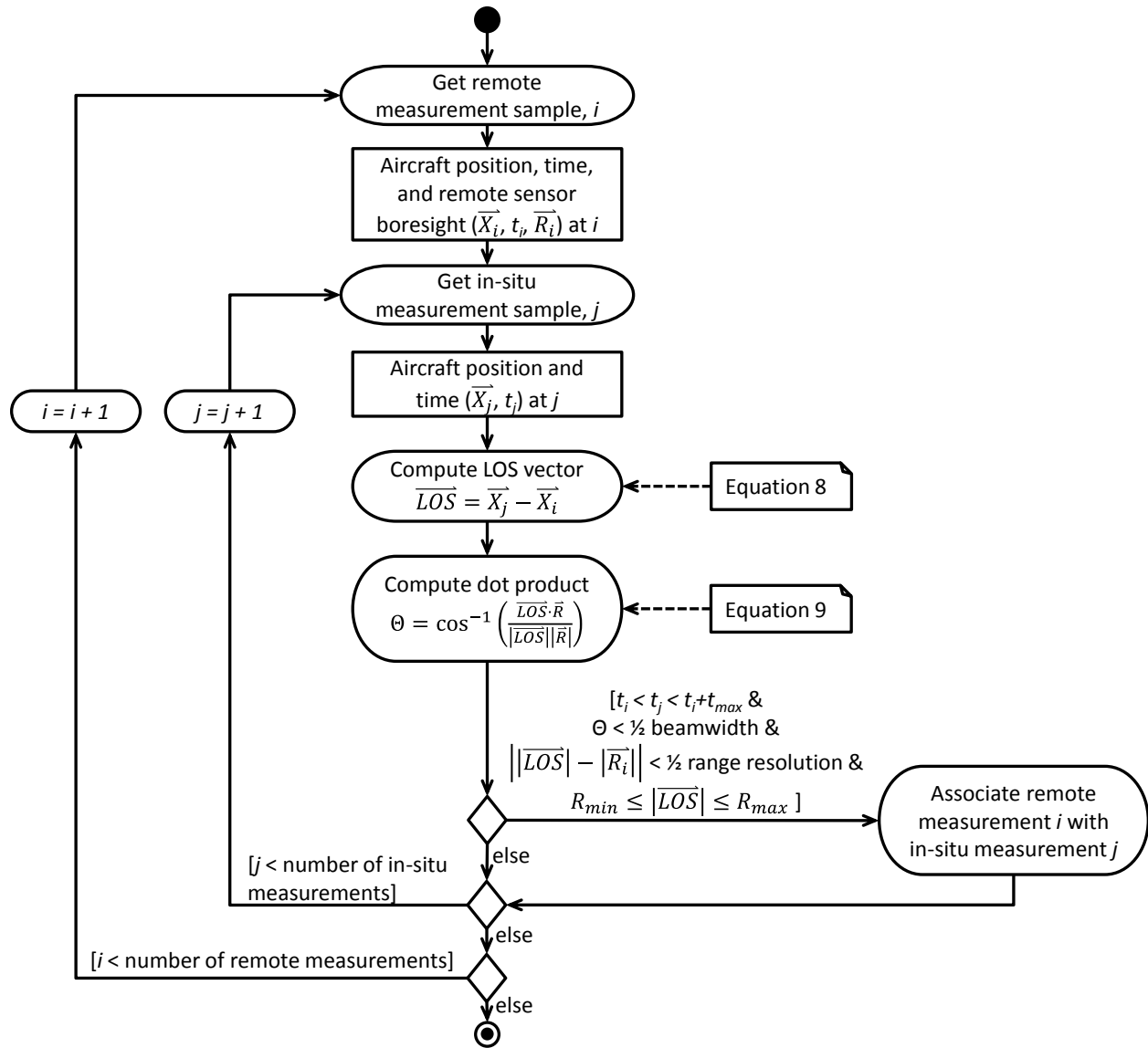


Figure 9: UML Activity Diagram of the Association Process

Combine to Match Distance Scale

At this point in the analysis process each in-situ measurement will be associated with a set of zero to many candidate remote measurements. A set of candidate remote measurements may contain remote measurements from overlapping boresight directions within a scan and from several different scans in the scan volume. To simplify the correlation results, the candidate associations are combined to produce a one-to-one relationship where a single representative remote measurement value correlates with a representative in-situ measurement (both with similar distance scales). The candidate remote measurements go through a two-step combination process (Figure 10). First, candidate remote measurements that come from overlapping remote sensor beams within a scan are combined in azimuth (i.e. beamwidth averaging). Second, the remaining candidate associations are combined to match distance scales between the remote and in-situ measurements.

The final step in the combination process reduces the remaining multiple candidate associations to a single

correlation for a single range of the remote sensor. The candidate associations are combined in a way that aims to match distance scale (i.e. in-situ sampling separation comparable to remote measurement resolution). One way to combine the candidate associations is by using the mean ignoring the relative quality of each remote measurement. Alternatively, the signal-to-noise ratio (SNR) provides a means to include the quality of each remote measurement. Regardless, combining the candidate remote measurements accounts for the spacing of the in-situ measurements for the comparison between remote and in-situ measurements to be spatially equivalent. The center value of a running mean of all in-situ measurements spanning a specific distance scale – representative of the range resolution of the remote sensor – is correlated with the (weighted or unweighted) mean of all candidate remote measurements associated with those same in-situ measurement positions.

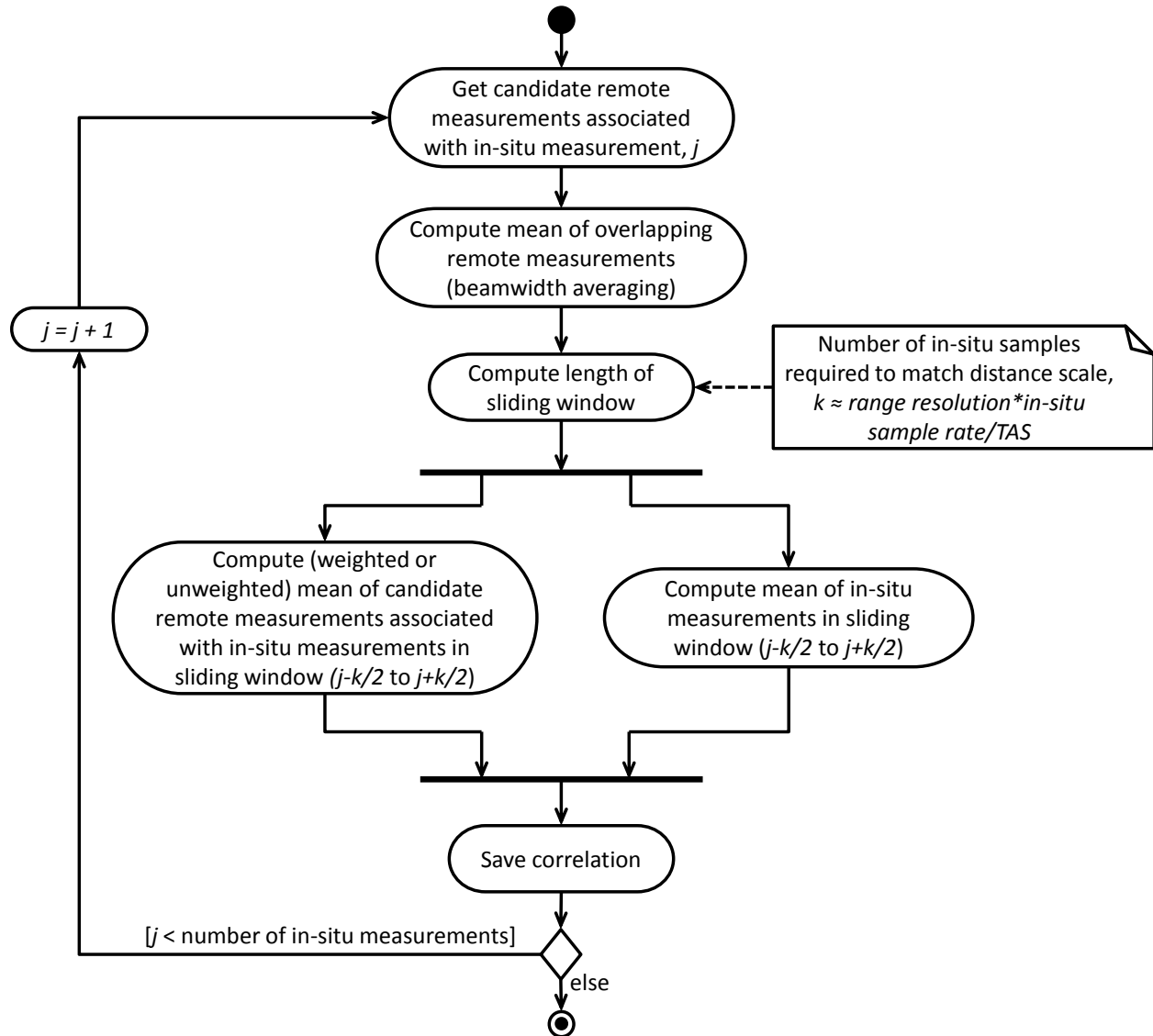


Figure 10: UML Activity Diagram of the Combination Process

The length of the sliding window is chosen to best match the distance scale of the in-situ measurements with the resolution volume of the remote sensor. The association process results in candidate measurements from the remote sensor located at each of the in-situ measurement positions. The number of candidate

associations combined to create a single representative value is dependent on two factors: how many candidate remote measurements are associated with each in-situ measurement, and how many in-situ measurement samples are included to match the distance scale. The ratio of the product of the remote sensor range resolution and the in-situ instrument sample rate to the aircraft true airspeed (i.e., *number of in-situ samples* \approx *range resolution* * *in-situ sample rate* / *TAS*) determines the number of in-situ samples included in the sliding window.

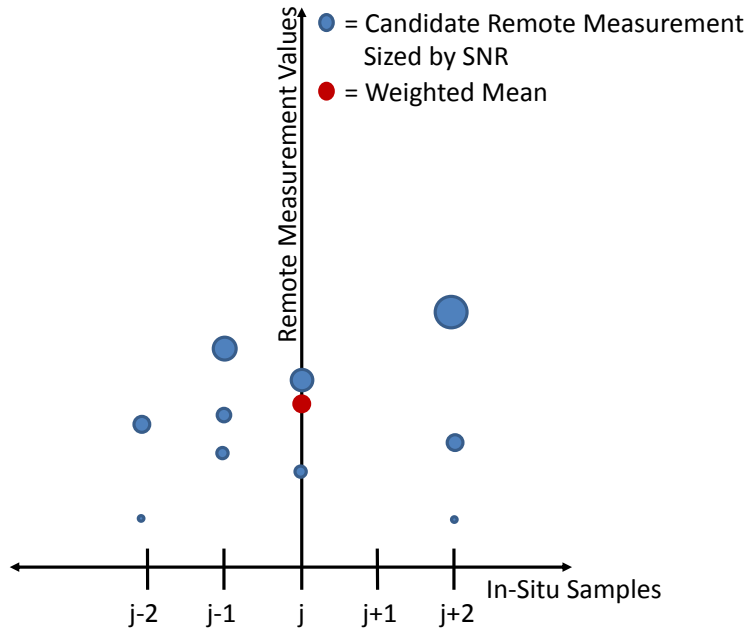


Figure 11: SNR Weighted Averaging of Candidate Remote Measurements to Match Distance Scale with In-situ Measurements

For example (Figure 11), if in-situ measurements are collected at 1 Hz intervals from an aircraft flying at 200 m/s TAS, then five in-situ measurements are required to represent an equivalent distance as a remote measurement with 1 km range resolution. In this case, applying a five-sample moving mean to the in-situ measurements with the corresponding (SNR-weighted) mean of all candidate remote measurements associated with the five in-situ samples, results in a one-to-one correlation between remote and in-situ measurements with comparable spatial resolution.

Sources of Uncertainty

The time between a remote measurement and an in-situ measurement of the same location contributes to uncertainty of the two measurements being representative of the same conditions. For remote measurements made at appreciable distances, tens of minutes may elapse (depending on the platform airspeed) before a corresponding in-situ measurement. Atmospheric changes over such time scales can be significant.

Additionally, the resolution volume of remote sensor measurements increases with range proportional to the beamwidth. While the correlation process considers range resolution when matching distance scales to in-situ measurements, it cannot compensate for angle resolution. For remote measurements made at appreciable distances, the vertical and lateral extent of a resolution volume may exceed thousands of meters; whereas in-situ instrument sample volumes are typically centimeter- up to meter-sized lateral dimensions. The constituent differences in these two sample volumes can lead to significant differences in their comparative measurements.

Likewise, atmospheric changes over the vertical and lateral extent of the remote sensor resolution volume can be significant for measurements made at farther ranges. Weather conditions can vary significantly over thousands of meters, especially in the vertical dimension. At many ranges well within the operational capabilities of current remote sensors, a resolution volume may encompass altitudes from the surface up to and beyond the Stratosphere. This contributes to uncertainty that the correlated remote and in-situ measurements are representative of the same weather conditions.

In general, remote measurements made at close range (nearest to and directly in front of the aircraft) will have the shortest time and smallest sample volume discrepancies with their associated in-situ measurements. Remote measurements made at close ranges from a swiftly moving platforms minimize beam spreading and allow little time to elapse before corresponding in-situ measurements are made, meaning these sources of error may be negligible (i.e. less than the uncertainty of the individual instruments). Conversely, slow platforms, long ranges, and wide beamwidths combine to produce significant temporal and spatial discrepancies such that the remote and in-situ measurements cannot be reasonably compared. Quantification of these uncertainties is highly scenario specific and may range from insignificant to unacceptable. However, the purpose of remote sensors is to measure conditions far ahead of an aircraft to provide advance information with sufficient time to allow decisions and actions to be performed based upon the remote measurements prior to encountering the conditions. Operational remote sensor systems must contend with these uncertainties.

Conclusion

A process has been described that allows correlation of remote measurements with in-situ measurements for sensor systems installed on a common flying platform. The correlation process makes use of geographic coordinate systems and conversions between them to solve the spatial associations. Temporal information is only used as a coarse filter to eliminate inappropriate associations. It is easily applied to recorded measurement data when the entire flight path is known. It cannot be applied in real-time during flight without a time delay and data buffering to account for the time difference between remote and in-situ measurements.

References

1. Ratvasky, T., Harrah, S., Strapp, J.W., Proctor, F. et al., “Summary of the High Ice Water Content (HIWC) Radar Flight Campaigns,” SAE Technical Paper 2019-01-2027, 2019, doi:10.4271/2019-01-2027.
2. Ratvasky, T., Harrah, S., Strapp, J.W., Proctor, F. et al., “Summary of the High Ice Water Content (HIWC) Radar Flight Campaigns,” NASA Report GRC-E-DAA-TN66897, June 17, 2019, <https://ntrs.nasa.gov/search.jsp?R=20190026988>
3. Harrah, S., Strickland, J., Hunt, P., Proctor, F. et al., “Radar Detection of High Concentrations of Ice Particles – Methodology and Preliminary Flight Test Results,” SAE Technical Paper 2019-01-2028, 2019, doi:10.4271/2019-01-2028.
4. Harrah, S., Strickland, J., Hunt, P., Proctor, F. et al., “Radar Detection of High Concentrations of Ice Particles – Methodology and Preliminary Flight Test Results,” NASA Technical Publication NF1676L-34421, NASA/TP-2019-220433, DOT/FAA/TC-19/29, L-21059, September 16, 2019, <https://ntrs.nasa.gov/search.jsp?R=20200000699>
5. Coordinate Systems Class Libray, NASA Software Catalog, LAR-19767-1, <https://software.nasa.gov/software/LAR-19767-1>
6. Coordiante-systems-class-library, NASA public GitHub, <https://github.com/nasa/Coordinate-systems-class-library>.
7. National Geospatial-Intelligence Agency (NGA) Standardization Document, World Geodetic System 1984, Version 1.0.0, 08 July 2014. NGA.STND.0036_1.0.0_WGS84.
8. Unified Modeling Language: <https://www.uml.org/>
9. Doxygen: <http://www.doxygen.nl/>

Abbreviations and Nomenclature

Abbreviation	Definition
AER	Azimuth-Elevation-Range
DCA	Down Range-Cross Range-Above
DCM	Direction Cosine Matrix
ECEF	Earth-Centered-Earth-Fixed
ECF	Earth-Centered-Fixed
ENU	East-North-Up
FAA	Federal Aviation Administration
GPS	Global Positioning System
HIWC	High Ice Water Content
LLA	Latitude-Longitude-Altitude
LOS	Line of Sight
NASA	National Aeronautics and Space Administration
PPI	Plan-Position Indicator
RRF	Radar Reflectivity Factor
SNR	Signal-to-Noise Ratio
TAS	True Airspeed
UML	Unified Modeling Language
WGS84	World Geodetic System 1984

Appendix

A software library consisting of a set of C++ classes was developed to compute the conversions between the coordinate systems. The class definitions are described by the UML class diagram (Figure 12) below. The library of classes represent various coordinate systems and provide the transformations between them. Abstract base classes are used to promote code reuse through inheritance. Coordinate systems represented are: East-North-Up (ENU), Downrange-Crossrange-Above (DCA), Latitude-Longitude-Altitude (LLA), Earth-Centered-Fixed (ECF), and Azimuth-Elevation-Range (AER). The software is included in the NASA software catalog [5] and the source code is publically available on GitHub [6]. Doxygen [9] compliant documentation is included.



Figure 12: Coordinate Systems UML Class Diagram

REPORT DOCUMENTATION PAGE

Form Approved
OMB No. 0704-0188

The public reporting burden for this collection of information is estimated to average 1 hour per response, including the time for reviewing instructions, searching existing data sources, gathering and maintaining the data needed, and completing and reviewing the collection of information. Send comments regarding this burden estimate or any other aspect of this collection of information, including suggestions for reducing the burden, to Department of Defense, Washington Headquarters Services, Directorate for Information Operations and Reports (0704-0188), 1215 Jefferson Davis Highway, Suite 1204, Arlington, VA 22202-4302. Respondents should be aware that notwithstanding any other provision of law, no person shall be subject to any penalty for failing to comply with a collection of information if it does not display a currently valid OMB control number.
PLEASE DO NOT RETURN YOUR FORM TO THE ABOVE ADDRESS.

1. REPORT DATE (DD-MM-YYYY) 01-06-2020		2. REPORT TYPE Technical Memorandum		3. DATES COVERED (From - To)	
4. TITLE AND SUBTITLE A Method for Correlating Forward-Looking Remote Sensor Measurements with In-Situ Measurements on Flying Platforms				5a. CONTRACT NUMBER	
				5b. GRANT NUMBER	
				5c. PROGRAM ELEMENT NUMBER	
6. AUTHOR(S) Strickland, Justin Kyle; Hunt, Patricia J.; Harrah, Steven D.; Switzer, George F.				5d. PROJECT NUMBER	
				5e. TASK NUMBER	
				5f. WORK UNIT NUMBER 80LARC17C0003	
7. PERFORMING ORGANIZATION NAME(S) AND ADDRESS(ES) NASA Langley Research Center Hampton, VA 23681-2199				8. PERFORMING ORGANIZATION REPORT NUMBER	
9. SPONSORING/MONITORING AGENCY NAME(S) AND ADDRESS(ES) National Aeronautics and Space Administration Washington, DC 20546-0001				10. SPONSOR/MONITOR'S ACRONYM(S) NASA	
				11. SPONSOR/MONITOR'S REPORT NUMBER(S) NASA/TM-2020-5002898	
12. DISTRIBUTION/AVAILABILITY STATEMENT Unclassified Subject Category : Availability: NASA STI Program (757) 864-9658					
13. SUPPLEMENTARY NOTES					
14. ABSTRACT A method is described for correlating measurements from a forward looking remote sensor with measurements made by in-situ instruments installed on the same flying platform. This method assumes that remote measurements are made within a volume of space in advance of the aircraft and that in-situ measurements provide representative values for discrete segments along the flight path. This correlation method can be applied to multiple sensors and makes no assumptions about the type of remote sensor or in-situ instrument, nor what either measures. It may be applied to recorded data during post-flight analysis based on known 4-D location (geospatial position and time) measurements.					
15. SUBJECT TERMS					
16. SECURITY CLASSIFICATION OF:			17. LIMITATION OF ABSTRACT	18. NUMBER OF PAGES	19a. NAME OF RESPONSIBLE PERSON
a. REPORT	b. ABSTRACT	c. THIS PAGE			STI Help Desk (email: help@sti.nasa.gov)
U	U	U	UU	22	19b. TELEPHONE NUMBER (Include area code) (757) 864-9658